

A Fast Local Bus Current-Based Primary Relaying Algorithm for HVDC Grids

Sahar Pirooz Azad, *Member, IEEE* and Dirk Van Hertem, *Senior Member, IEEE*

Abstract—This paper proposes a fast, selective, reliable and local bus primary relaying algorithm for high voltage direct current (HVDC) grids. The proposed relaying algorithm only uses measurements obtained from current sensors to detect faults and identify their locations. This algorithm is local and requires only communication at the bus level rather than system level. Furthermore, the algorithm is not sensitive to system configuration and operating point and can be employed during line or converter outages with limited re-tuning and adjustments.

The proposed algorithm is applied to a four-terminal HVDC grid. Study results show that the proposed algorithm i) detects faults on both transmission lines and DC buses, ii) identifies the faulted bus or transmission line, iii) requires insignificant computation capacity, iv) distinguishes between faults and other system transients to prevent erroneous circuit breaker trips, and v) is not sensitive to measurement noise.

Index Terms—protective relaying, HVDC transmission lines, power system protection

I. INTRODUCTION

To achieve a more sustainable energy system, more renewable energy resources are being added to the power system. The integration of renewable resources such as offshore wind requires a transformation of the existing power system. One approach is to expand the existing point-to-point high voltage direct current (HVDC) transmission lines to multi-terminal HVDC networks and potentially HVDC grids [1]; as HVDC technology is the only solution for economic power transmission over long distances and cable connections [2].

An HVDC grid, where multiple DC converters are interconnected by a meshed DC transmission network, is envisioned to play a significant role in the future smart grid. Several challenges, in particular, those associated with control and protection, have hindered the realization of HVDC grids. HVDC grid protection is far more difficult than AC grid protection as DC fault phenomenon is one order of magnitude faster than AC fault phenomenon.

An HVDC grid protection system consists of DC circuit breakers, relaying algorithm and sensors. In recent years, there have been significant advancements in developing fast DC breakers, e.g., electro-mechanical, pure solid-state and hybrid [3]. However, fast, selective, reliable and sensitive relaying algorithms, in the order of milliseconds, are still required to quickly detect the fault and identify its location [4].

A comprehensive review of relaying algorithms for multi-terminal HVDC grids is provided in [5]. The existing relays include derivatives [6], voltage and current differential [7],

[8], overcurrent [9], [10] and traveling wave [11]. Derivative relays use the rate of rise of current or voltage measurement for fault detection and their speed relies on the accuracy of the derivative signals and the time required to mitigate the high frequency effects in the waveforms. Overcurrent relays are mostly used for blocking of converter valves or backup protection. Their application as selective primary relays is limited [9]. Traveling wave-based relays rely on the detection of a steep initial wavefront in the voltage signal [4], [12]. These algorithms primarily use measurements from voltage sensors to detect faults and require high bandwidth voltage sensors at the ends of all transmission lines. These algorithms also require measurements obtained from current sensors to distinguish between faults on DC buses and transmission lines, as voltage measurements do not contain such information. Therefore, these relaying algorithms based on voltage measurements require both current and voltage sensors and are less economically viable compared to algorithms relying only on current measurements. Those algorithms relying on only voltage measurements require additional voltage sensors at the two ends of all current limiting inductors to detect bus faults [8], [13]. Newly-developed distance relays for DC protection also require two voltage divider measurements [14] or both current and voltage measurements [15] to detect faults on transmission lines. Furthermore, a number of the proposed relaying algorithms such as voltage and current differential require communication between relays at both ends of transmission lines [14], [16]–[19]. These algorithms may suffer from communication complexities due to time delays and noise and requires excessive communication infrastructure for large HVDC grids. DC Protection schemes using AC breakers such as the handshaking method [20] also use current measurements to detect faults on transmission lines, however such methods result in the loss of the entire grid during fault detection and isolation.

This paper proposes a local bus primary relaying algorithm based on measurements obtained only from current sensors. There are several features associated with the proposed algorithm: The algorithm 1) detects faults both on DC buses and HVDC transmission lines, 2) does not require costly voltage sensors for fault detection and identification, 3) is local as it only requires communication at the DC bus level, 4) is computationally inexpensive, 5) is not sensitive to the system operating point, 6) distinguishes between transients caused by faults and other events such as line or converter outages, 7) does not generate erroneous and unnecessary trip signals due to the trip of responsible breakers, and 8) is not sensitive to measurement noise.

This paper describes the design procedure of the proposed

S. Pirooz Azad is with the Department of Electrical and Computer Engineering, University of Alberta, Edmonton, AB, Canada and D. Van Hertem is with the Electrical Engineering Department of KU Leuven, Leuven, Belgium (e-mail: spazad@ualberta.ca; dirk.vanhertem@esat.kuleuven.be)

primary relaying algorithm and evaluates its performance for detecting both pole-to-pole and pole-to-ground faults on DC buses and transmission lines. The relaying algorithm is applied to a four-terminal HVDC grid with a symmetrical monopole configuration. Study results show that the algorithm possesses all the aforementioned features and promptly and accurately detects faults under various system operating points and outages.

The remainder of the paper is organized as follows: The study system is presented in Section II. The primary relaying algorithm is discussed in section III. Case studies, simulation results and discussions are presented in section IV. Conclusions are provided in section V.

II. TEST SYSTEM

The test system considered in the studies of this paper is the four-terminal meshed HVDC grid of [21], Fig. 1a. The test system represents a cable-based meshed HVDC grid connecting two offshore wind farms to two onshore AC systems.

A. HVDC Grid Components

Half-bridge modular multilevel converters with symmetric monopole configuration (with a DC voltage of ± 320 kV) are connected to all DC terminals. A neutral point is available at the DC side of all converters by using DC capacitors. The neutral point is solidly grounded. The converters are presented by a continuous model with anti-parallel diodes to represent their IGBT blocking capability [22]. The cables are represented with a frequency-dependent distributed parameter model. The cable characteristic impedance (at 1 MHz) is 33.1 Ω and the traveling wave velocity is 183.5 km/ms.

The detailed description of the test system component models and parameters is given in [21]. All the AC and DC system parameters are similar to those of [21], except for the series inductors which are considered to be 50 mH.

B. Breakers and Sensors

Fig. 1b shows the location of transducers and breakers. Fast breakers CB_{ij} and CB_i are respectively inserted at ends of all transmission lines and the DC side of converters. Inductors L_s are placed in series with breakers to limit the rate of rise of current. Current sensors S_{Bi} and S_{ij} are located between inductors and circuit breakers, Fig. 1b. White Gaussian noise is added to all signals to represent the various sources of noise that can be introduced by the sensing elements, electronic units and signal processing components of the current sensors.

Fig. 2 shows the model of the breaker used in the studies of this paper [23]. In this model, the current flows through load commutation switches during normal conditions. After the breaker receives the trip signal, the load commutation switches open and, within 250 μ s, commutate the fault current into the main breaker [23]. Thereafter, the ultrafast disconnecter opens within 2 ms and disconnects the load commutation switches from the main circuit. Then, the main breaker opens and commutates the fault current into the surge arrester bank. The

surge arrester bank dissipates the fault energy and reduces the fault current into zero. After the fault current is interrupted, the residual current breaker opens within 1 s to protect the arrester bank from thermal overload. The proposed relaying algorithm of this paper can be used with any type of fast breaker and its application is not limited to the described hybrid breaker.

III. PRIMARY RELAYING ALGORITHM

The proposed primary relaying algorithm consists of several fault detection and identification (FDI) units, where each one is associated with one DC bus, Fig. 3. The inputs to unit i are the measurements from sensors S_{Bi} and S_{ij} . In each FDI unit, a local bus relaying algorithm is applied to the unit inputs and trip signals T_i and T_{ij} are generated. T_i and T_{ij} trigger the trip of CB_i and CB_{ij} , respectively. The relaying algorithm of each FDI unit is a local one as only measurements at the bus level are used to detect faults.

Each FDI unit includes three types of modules: i) bus fault detection, ii) line fault detection, and iii) breaker coordination, Fig. 4. Each FDI unit has one bus fault detection module, one breaker coordination module and N line fault detection modules, where N is the number of transmission lines connected to the associated DC bus.

To protect an HVDC grid, for a line fault, only breakers at ends of the faulted line should trip. However, for a fault at a DC bus, all breakers connected to that bus should trip. An alternative is to replace the breaker at the DC side of a converter with a disconnecter. To clear a bus fault in such a configuration, the breaker at the AC side of the converter trips. Then, the disconnecter at the DC side of the converter opens to de-energize both the DC bus and the converter. In this paper, it is assumed that a breaker is located at the DC side of each converter. This configuration expedites the restoration of the grid.

A. Bus Fault Detection Module

The input to the bus fault detection module of FDI unit i includes measurements from sensors S_{Bi} and S_{ij} ($j \in C_i$ where C_i corresponds to the set of all lines connected to bus i), Fig. 4. In the bus fault detection algorithm, the absolute value of sum of all inputs to the module (SB_i), is compared against a threshold I_{TH}^B , Fig. 5. $SB_i = \sum_{j \in C_i} I_{ij} + I_i$ where I_{ij} and I_i are the currents measured by S_{ij} and S_{Bi} , respectively. If $|SB_i| > I_{TH}^B$, a bus fault is detected. A near-zero value can be selected for I_{TH}^B to discriminate between line and bus faults as well as accounting for measurement noise.

Since the bus fault detection algorithm uses measurements from all connections to the bus, it can correctly detect DC bus faults and does not misidentify line faults close to the bus as bus faults. Discriminating between bus and line faults is particularly necessary for scenarios in which a line fault occurs close to the bus. In such scenarios, the measurements at the healthy lines adjacent to the faulted line do not differ significantly from those of scenarios with a bus fault. Therefore, with an improper relaying algorithm, line faults close to buses might be misidentified as bus faults and erroneous trip signals might be sent to breakers.

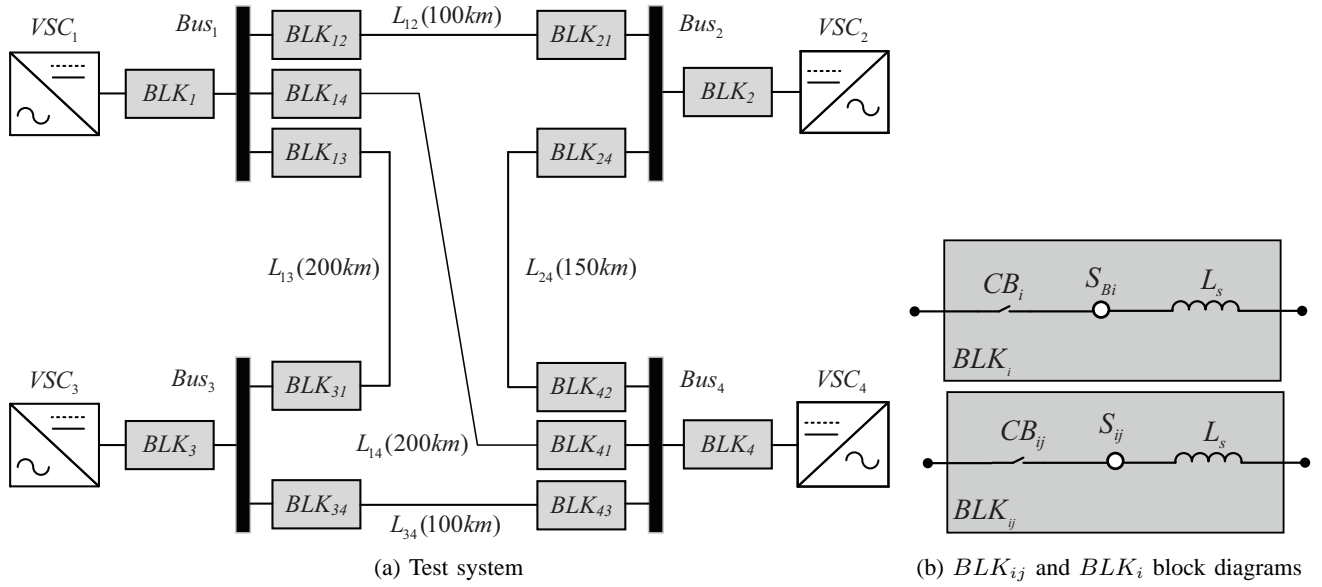


Fig. 1: Four-terminal meshed HVDC grid test system

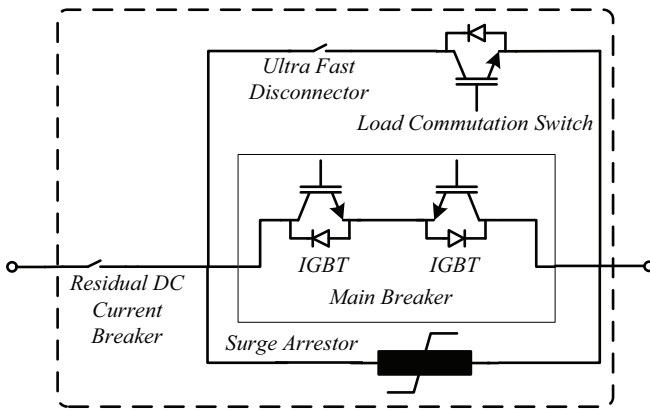


Fig. 2: Hybrid DC circuit breaker [3]

B. Line Fault Detection Module

The input to the line L_{ij} fault detection module of FDI unit i is the current measurement of sensor S_{ij} , Fig. 4. In this module, a new signal $\bar{d}I_{ij}$ is generated from the current measurement I_{ij} . $\bar{d}I_{ij}$ is the deviation of I_{ij} from its moving average with a window size of 20 samples ($\bar{d}I_{ij} = I_{ij} - MA(I_{ij})$, where $MA(\cdot)$ stands for moving average). In the line fault detection module, three criteria are evaluated, Fig. 5: i) potential fault, ii) reliability, and iii) selectivity. If all three criteria are satisfied, a line fault is detected.

The potential fault criterion is satisfied and a potential fault on L_{ij} is identified, when a peak in $\bar{d}I_{ij}$ is detected. A peak is only detected if the local extremum of $\bar{d}I_{ij}$ remains the maximum for more than two consecutive samples. This will prevent the misidentification of local maximums caused by measurement noise as a peak resulted from a fault. The value of I_{ij} at the instant that the n^{th} peak of $\bar{d}I_{ij}$ is detected, is denoted by I_{ij}^n .

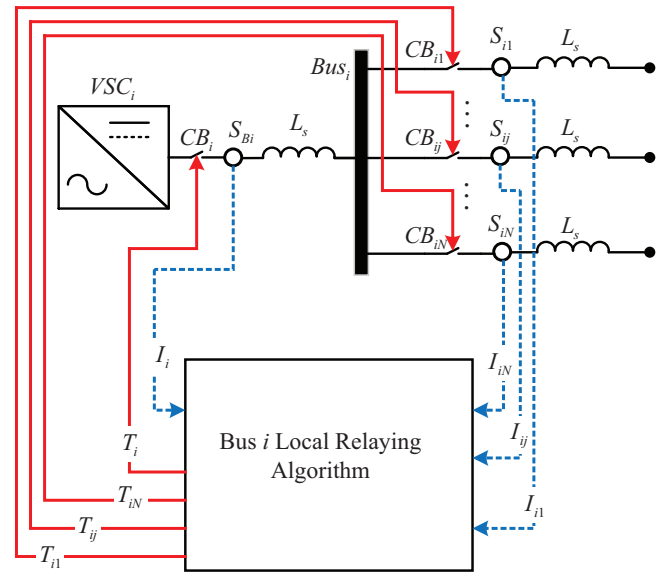


Fig. 3: DC bus i layout and its associated FDI unit

In HVDC grids, regardless of the configurations or grounding types, a DC fault always results in an increase in the fault current and consequently a peak in $\bar{d}I_{ij}$. As the proposed algorithm relies on detecting a peak in $\bar{d}I_{ij}$ to identify a potential fault, it can be applied to grids with various configurations including symmetric monopole, asymmetric monopole, bipole as well as grids with various grounding type.

The reliability criterion is required to prevent the false trip of breakers in case of transients other than faults, i.e., converter and line outages or trip of responsible breakers. In the reliability criterion, I_{ij}^n is compared against max_{ij} . max_{ij} is the maximum value of I_{ij} at instants that a peak of $\bar{d}I_{ij}$ is detected. If $I_{ij}^n \geq max_{ij}$, the reliability criterion is satisfied.

When both potential fault and reliability criteria are sat-

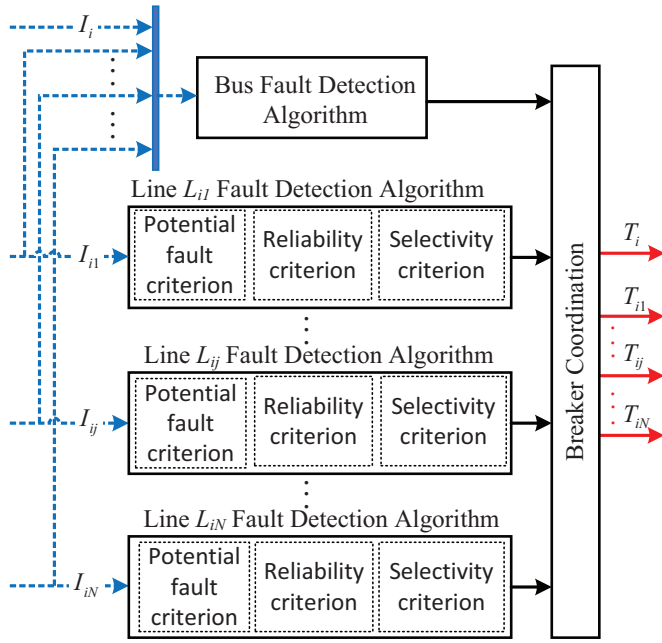


Fig. 4: FDI unit associated with DC bus i

ified, the selectivity criterion is evaluated. In the selectivity criterion, $\bar{d}I_{ij}$ is compared against a threshold I_{TH}^L . If $\bar{d}I_{ij} > I_{TH}^L$, the selectivity criterion is satisfied. The selectivity criterion is required to distinguish between faults on line L_{ij} and other lines. The threshold value I_{TH}^L can be selected as any value between the minimum value of $\bar{d}I_{ij}$ for faults on L_{ij} (F_{ij1}) and the maximum value of $\bar{d}I_{ij}$ for faults on adjacent lines to L_{ij} . This threshold can be calculated using a simulation study evaluating faults on the line to be protected and nearby lines. The selectivity requirement of any relaying algorithm necessitates that a breaker should only trip if a fault occurs on the line where it is located. If the selectivity criterion is satisfied, an actual line fault is detected. If the selectivity criterion associated with line L_{ij} is not satisfied, the potential fault will not be identified as an existent fault on line L_{ij} . In such a case, a peak in $\bar{d}I_{ij}$ signal is detected due to a fault on adjacent lines to line L_{ij} .

C. Breaker Coordination Module

The breaker coordination module, depicted in Fig. 5, generates the trip signals for the responsible breakers. In this module, when a DC bus fault is detected, the trip signals T_i and T_{ij} for all breakers connected to the faulted bus become one. T_i and T_{ij} are associated with CB_i and CB_{ij} , respectively. When a line fault is detected, the trip signal for the breaker located at the faulted line becomes one. However, if the trip signal for an adjacent breaker is already one ($T_{ik} = 1$ for $k \in C_i$ and $k \neq j$), T_{ij} will remain zero. The goal is to further improve the reliability of the relaying algorithm and to prevent the false trip of breakers located at healthy lines adjacent to a faulted line. T_i and T_{ij} remain one until the fault is cleared.

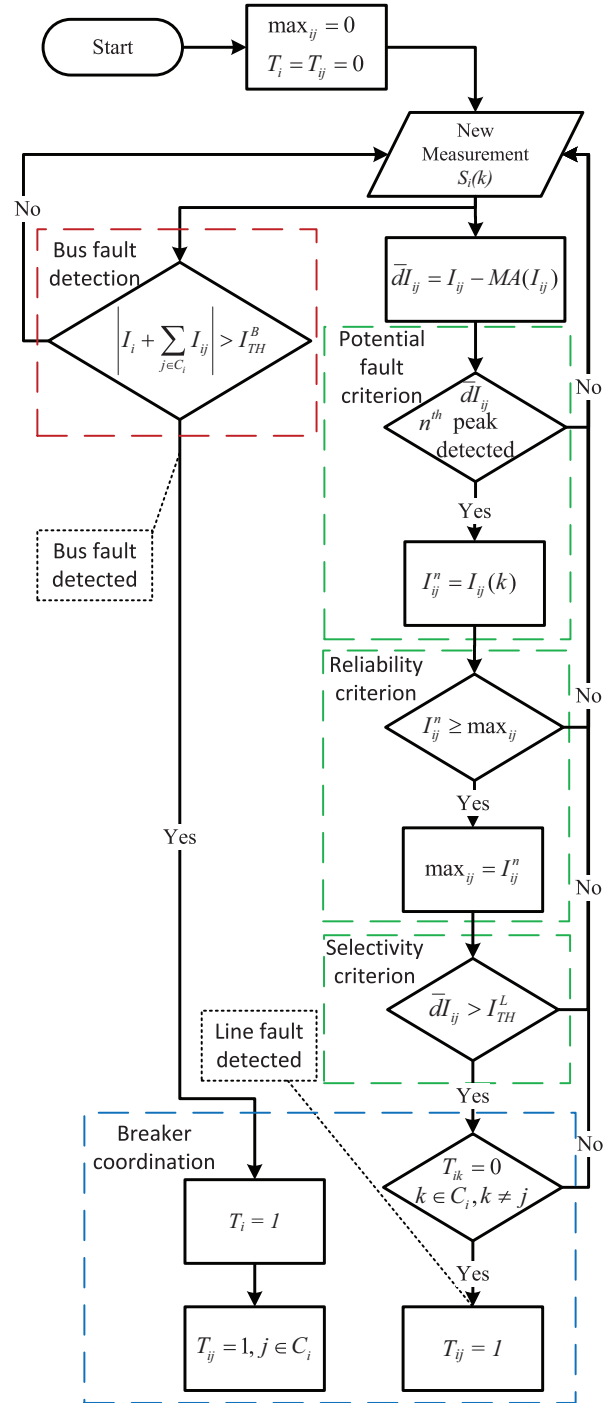


Fig. 5: Bus i relaying algorithm flowchart

IV. STUDY RESULTS

In this section, the performance of the proposed relaying algorithm in detecting bus and line faults and identifying the faulted bus or line is evaluated. Furthermore, the reliability of the proposed method during system disturbances, e.g., line and converter outages, is investigated. The faults considered in this study are permanent pole-to-pole and pole-to-ground faults which occur at 0 s. Faults at bus i and line L_{ij} are identified as F_{Busi} and F_{ijk} , respectively. In the latter notation, F_{ijk} refers to a fault on line L_{ij} at $(k - 1) * 25$ km from bus i , e.g., F_{ij1}

refers to a fault on line L_{ij} right after the series inductor. For each sensor S_{ij} , currents flowing from the bus toward a line are assumed to be positive. For each sensor S_{Bi} , the positive direction is from the DC bus toward the converter station. The sampling frequency is 50 kHz. For the studies of this paper, the test system of Fig. 1a is modeled in PSCAD [24].

A. Bus Faults

1) *Pole-to-Pole Faults*: Fig. 6 shows $|SB_3|$ for two pole-to-pole fault scenarios, i.e., F_{Bus3} and F_{311} . Fig. 6 shows that during F_{Bus3} , $|SB_3|$ is significantly greater than zero; whereas during F_{311} , it remains close to zero. Therefore, even a small threshold (I_{TH}^B) can be used to distinguish between bus and line faults. A nonzero value of I_{TH}^B is used to account for measurement noise.

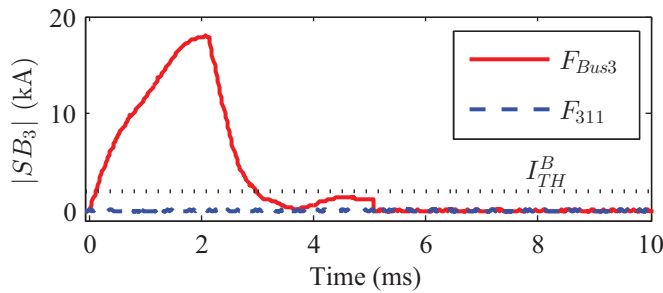


Fig. 6: $|SB_3|$ during pole-to-pole F_{311} and F_{Bus3} faults

After F_{Bus3} detection, trip signals are generated by the proposed relaying algorithm and breakers CB_{31} , CB_{34} and CB_3 open to disconnect all lines connected to the faulted bus, Fig. 7. Consequently, CB_{13} and CB_{43} trip to disconnect the lines connected to only one bus. The trip signals for breakers connected to buses 3, 1 and 4 are respectively generated at 0.1 ms, 1.6 ms and 2.6 ms. The time required to generate the trip signals consists of the time delay of the traveling fault wave to reach the sensors and the processing time for detecting the fault. For example, with a traveling wave speed of 183.5 km/ms, it takes 1.1 ms for the fault wave to reach the sensor at the remote end of the 200 km faulted line L_{13} . After the trip of breakers, the DC fault currents quickly reach zero and the maximum fault current that breakers interrupt is 6.5 kA, Fig. 8.

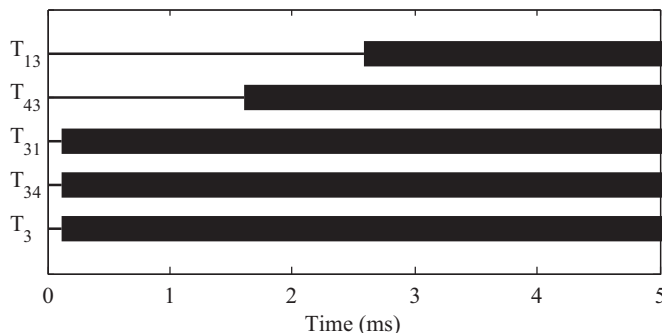


Fig. 7: Trip signals during the pole-to-pole F_{Bus3} fault

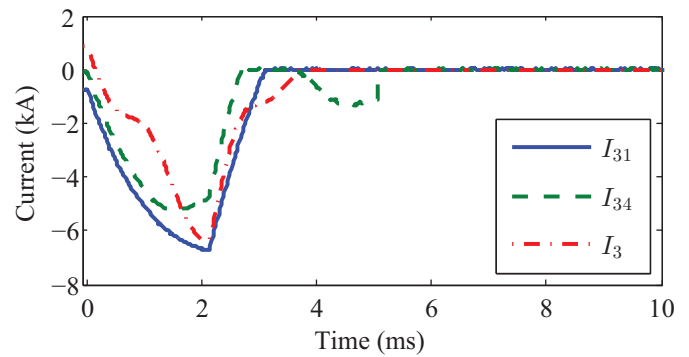


Fig. 8: Positive pole currents measured at bus 3 during the pole-to-pole F_{Bus3} fault

2) *Pole-to-Ground Faults*: For detecting pole-to-ground faults, the same algorithm as the one used for pole-to-pole faults is utilized. In a system which has converters with a symmetric monopole configuration, both faulted and healthy poles should be disconnected in case of a pole-to-ground fault. After the healthy cable is separated from the system, it should be discharged through the earthing switches, whereas the faulted cable will automatically discharge through the fault. In this paper, the healthy cable is discharged 5 ms after the main breaker interrupts the current.

For a positive pole-to-ground F_{Bus3} fault, the trip signals for breakers connected to bus 3 (CB_{31} , CB_{34} and CB_3), bus 1 (CB_{13}) and bus 4 (CB_{43}) for both positive and negative poles are respectively generated at 0.1 ms, 1.6 ms and 2.7 ms, Fig. 9. The maximum fault currents that breakers interrupt are respectively 6.55 kA and 2.7 kA for the positive and negative poles.

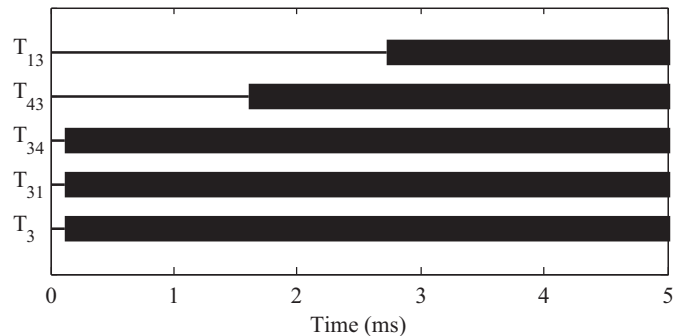


Fig. 9: Trip signals during the positive pole-to-ground F_{Bus3} fault

B. Line Faults

1) *Pole-to-Pole Faults*: In the proposed relaying algorithm, a moving window containing 20 samples (identified as a black rectangle on Fig. 10) passes along I_{31} to form dI_{31} . The new dI_{31} signal shown on Fig. 10 (b) is calculated at each sampling instant. In this figure, the filled circle markers on dI_{31} signal indicate the calculated samples associated with the moving window of Fig. 10 (a). Fig. 10 (c) is the zoomed view of

Figs. 10 (a)-(b). All signals depicted in Fig. 10 are associated with the fault scenario during which all breakers are disabled.

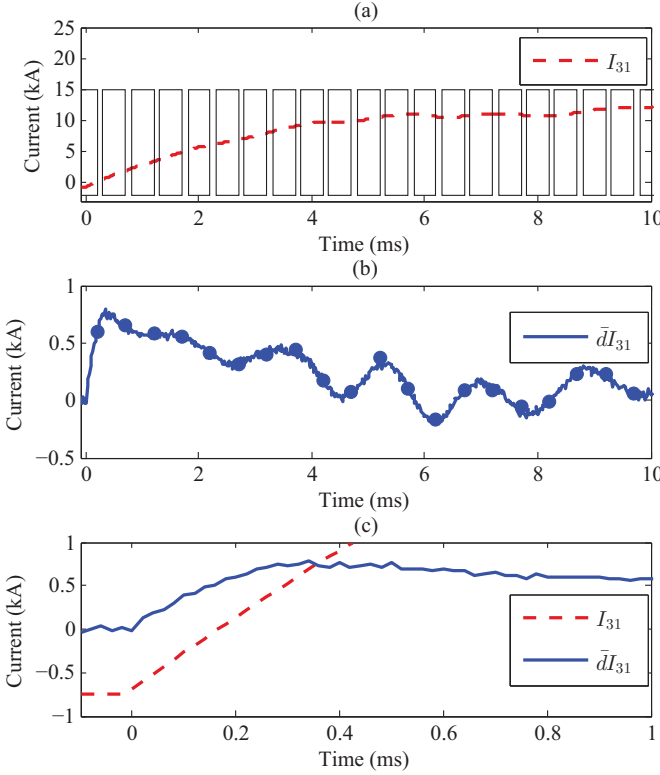


Fig. 10: (a) Positive pole I_{31} , (b) Positive pole $\bar{d}I_{31}$, and (c) Positive pole I_{31} and $\bar{d}I_{31}$ -during the pole-to-pole F_{311} fault (breakers are disabled)

Fig. 10 (c) shows that as $\bar{d}I_{31}$ reaches its peak, I_{31} remains below 1 kA. Therefore, a potential fault can be detected before the current reaches high values. This is one of the advantages of the proposed relaying algorithm over those methods relying on thresholds such as [4], where the current reaches higher values before the fault is detected. Furthermore, in such methods, the threshold should be specifically calculated for each system configuration and operating point. However, in the proposed algorithm, regardless of the system operating point or configuration, the peak of $\bar{d}I_{ij}$ corresponds to a potential fault. A number of relaying algorithms also use current derivatives for fault detection [4]. However, using a simple derivative of current measurements will compromise the relaying algorithm performance due to its exposure to intensified measurement noises.

During the pole-to-pole F_{311} fault, the current of the faulted line remains below 8 kA, Fig. 11 (a). The fault is detected at the two ends of the faulted line at 0.4 ms and 1.7 ms, Fig. 11 (c). Fig. 11 (c) shows that only breakers at the two ends of the faulted line trip and therefore, the selectivity criterion is satisfied. Five critical points can be derived from Fig. 11 (b), which illustrate how the proposed relaying algorithm successfully detects various faults and generates the trip signals for responsible breakers:

- 1) after a fault on line L_{ij} , $\bar{d}I_{ik}$ and $\bar{d}I_{jk}$ signals associated with the healthy lines adjacent to the faulted line (such

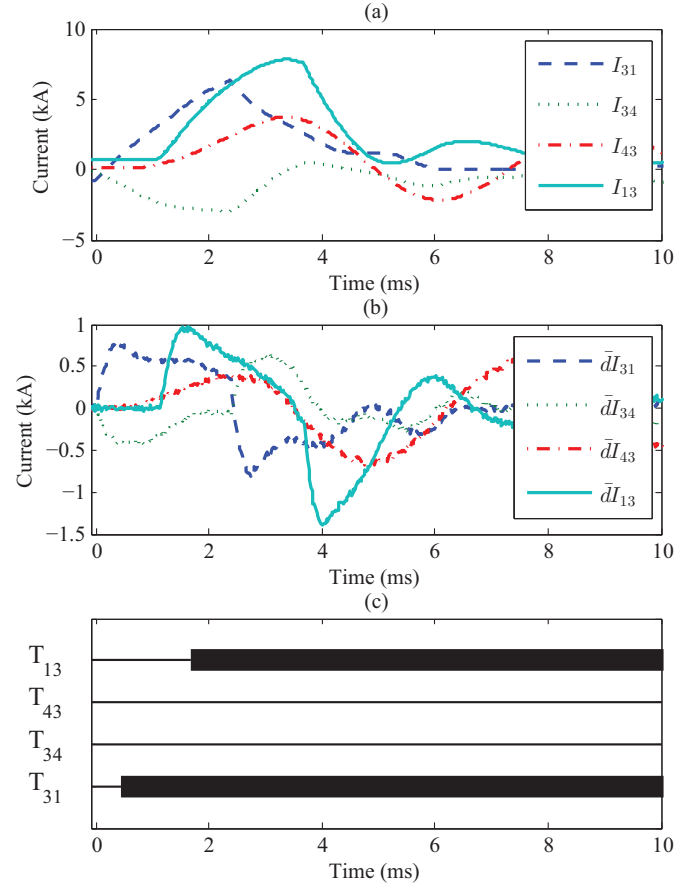


Fig. 11: (a) Positive pole currents, (b) Positive pole $\bar{d}I_{ij}$ currents, and (c) Trip signals-during the pole-to-pole F_{311} fault (breakers are enabled)

as $\bar{d}I_{34}$ in this example) will have negative values. The negative sign is due to the opposite direction of the fault wave in the healthy and faulted lines. The sign difference in $\bar{d}I_{ij}$ signals is used in the proposed relaying algorithm, in particular in the selectivity criterion, to distinguish between healthy and faulted lines connected to the same bus. Furthermore, the breaker coordination module of each bus does not allow the trip of more than one breaker connected to a bus.

- 2) $\bar{d}I_{ij}$ signal that primarily reaches its peak is associated with the sensor closest to the fault location. Therefore, the breaker closest to the fault location, i.e., CB_{31} , trips before the rest of breakers.
- 3) after the first breaker interrupts the current, the second $\bar{d}I_{ij}$ signal reaches its peak. Depending on system inductance values and length of transmission lines, this signal can be associated with the measurement at the remote end of either the faulted line or adjacent healthy lines. In the test system of this paper, $\bar{d}I_{13}$ reaches its peak before $\bar{d}I_{43}$ and CB_{13} is the second breaker to trip.
- 4) after trip signals are sent to breakers located at the faulted line, it takes them 2 ms to interrupt the fault current. Meanwhile, the fault wave travels to healthy lines. Therefore, $\bar{d}I_{ij}$ signals associated with measurements at remote

sensors reach their peak values. However, these peak values do not trigger the trip of any breakers. Fig. 11 (b)-(c) shows that as $\bar{d}I_{43}$ reaches its peak value, no trip signal for CB_{43} is generated due to the selectivity criterion.

- 5) $\bar{d}I_{34}$ signal eventually reaches a positive peak and $\bar{d}I_{43}$ signal reaches a second peak larger than the first one. None of these peaks triggers a breaker trip due to the reliability criterion.

In summary, a potential line fault is detected as the $\bar{d}I_{ij}$ signal associated with a measurement at the faulted line reaches its peak value. The rest of the local maximums observed in $\bar{d}I_{ij}$ signals do not lead to trip of any breakers. These peaks are the result of traveling fault waves or disturbances caused by the trip of breakers at the faulted line. Selectivity and/or reliability criteria prevent the unnecessary trip of breakers in the presence of such local maximums. Sections IV-C and IV-D discuss the advantages of the proposed selectivity and reliability criteria and explain how these criteria prevent the unnecessary trip of breakers.

2) *Pole-to-Ground Faults:* For detecting pole-to-ground line faults, the same algorithm as the one used for pole-to-pole line faults is employed. After a pole-to-ground fault detection, both healthy and faulted poles associated with the faulted line are removed and 5 ms after the main breaker interrupts the current, the voltage of the healthy pole is forced to zero.

During a positive pole-to-ground F_{311} fault, the trip signals for breakers CB_{13} and CB_{31} are respectively generated at 1.7 ms and 0.4 ms, Fig. 12. The maximum fault currents that breakers interrupt are 7.1 kA and 1 kA for the positive and negative poles, respectively, Fig. 13. Thereafter, due to the discharge of the capacitance associated with the faulted cable healthy pole, the breakers at the healthy pole will be exposed to 2.5 kA. However, these transients in the pole current do not result in any unnecessary breaker trips.

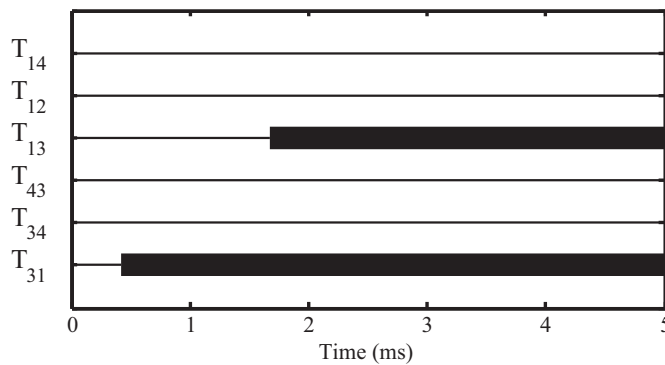


Fig. 12: Trip signals during the positive pole-to-ground F_{311} fault

C. Selectivity Evaluation

One of the advantages of using $\bar{d}I_{ij}$ for fault detection is the significant difference between its peak magnitude for faults on line L_{ij} and faults on other lines. Based on this peak magnitude difference, a simple selectivity criterion, i.e.,

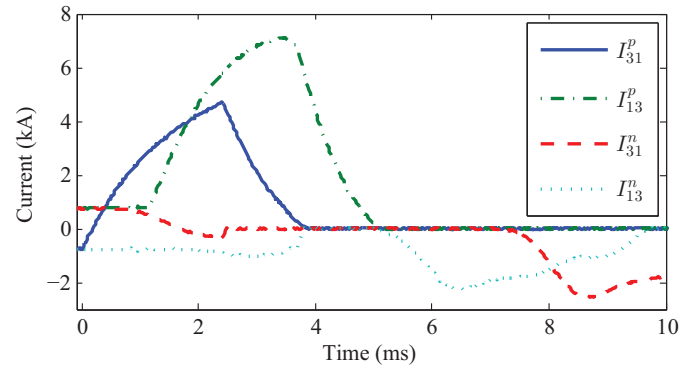


Fig. 13: Line L_{13} positive and negative poles current measurement during the positive pole-to-ground F_{311} fault

comparison against a threshold, is developed. As an example, $\bar{d}I_{43}$ for three fault scenarios, i.e., F_{311} , F_{341} and F_{345} , is depicted in Fig. 14. The maximum value of $\bar{d}I_{43}$ for any fault on line L_{34} is between those associated with faults F_{341} and F_{345} . F_{311} is the closest fault (on an adjacent line) to S_{43} , and it causes the highest amplitude positive peak in $\bar{d}I_{43}$ among faults occurring on lines other than L_{34} . Faults on lines connected to bus 4, other than L_{34} , primarily result in negative peaks in $\bar{d}I_{43}$. The magnitude of the first peak of $\bar{d}I_{43}$ for faults F_{311} , F_{345} and F_{341} are 0.4018, 0.9070 and 1.215, respectively. Therefore, to distinguish faults on L_{34} from those on other lines, any threshold value of I_{TH}^L between 0.4018 and 0.9017 can be selected.

In this paper, I_{TH}^L is considered to be 0.5. One advantage of the proposed relaying algorithm is that the selection of I_{TH}^L is straightforward as the minimum amplitude of the peaks of $\bar{d}I_{ij}$ (for faults on line L_{ij}) is almost twice its maximum value for faults on lines L_{jk} ($k \in C_j$, $k \neq i$). Another advantage of the proposed selectivity criterion is that it does not require fault currents to reach pre-defined thresholds and therefore, identifies faults while fault currents can be interrupted by breakers.

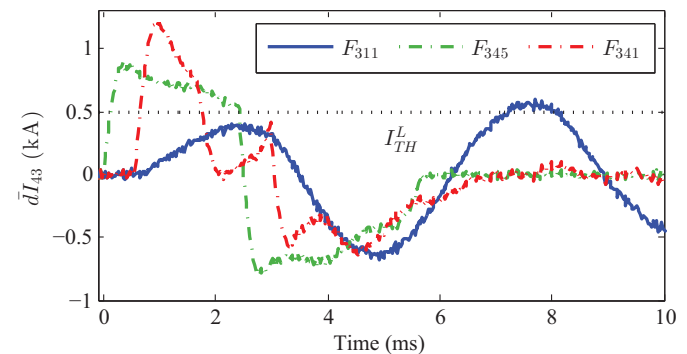


Fig. 14: $\bar{d}I_{43}$ during pole-to-pole F_{311} , F_{341} and F_{345} faults

D. Reliability Evaluation

This section evaluates the performance of the proposed algorithm in discriminating between faults and other system disturbances. Three types of disturbances, i.e., line and converter outages and trip of responsible breakers are investigated.

1) *Trip of Responsible Breakers*: Any relaying algorithm should be designed such that the trip of responsible breakers are not misinterpreted as a fault. In Fig. 14, although the first peak of $\bar{d}I_{43}$ does not reach I_{TH}^L during F_{311} , the second peak does. This is due to the trip of breakers located on the faulted line, Fig. 15. If breakers located on L_{31} remain closed, the peak of $\bar{d}I_{43}$ will not exceed I_{TH}^L . Although the selectivity criterion is satisfied in this fault scenario, the reliability criterion ensures that such peaks do not result in any unnecessary breaker trips. Selecting a higher I_{TH}^L does not solve the problem as it might jeopardize the selectivity of the algorithm or may result in fault detection failure.

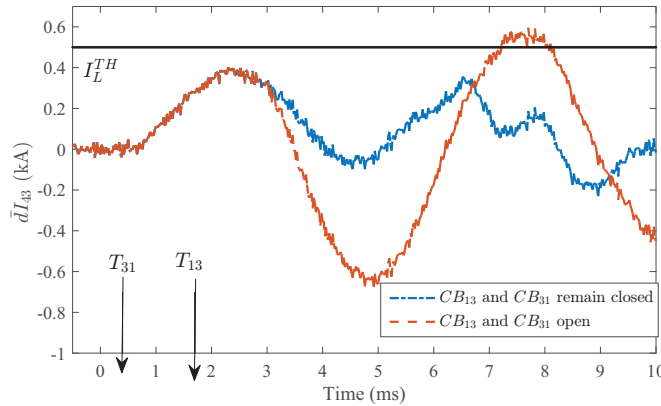


Fig. 15: $\bar{d}I_{43}$ during the pole-to-pole F_{311} fault

The proposed reliability criterion identifies a potential fault as an actual one if the peak of $\bar{d}I_{ij}$ occurs as I_{ij} is not oscillating, albeit increasing toward a steady-state value. Fig. 16 shows that the second peak of $\bar{d}I_{43}$, which exceeds I_{TH}^L , occurs as I_{43} is oscillating. Therefore, based on the reliability criterion, only the first peak of $\bar{d}I_{43}$ corresponds to an existent fault. To distinguish the first peak of $\bar{d}I_{43}$ from the other ones, I_{43}^n is compared against max_{43} . I_{43}^n is the amplitude of I_{43} at the instant the n^{th} peak of $\bar{d}I_{43}$ is detected. In this fault scenario, $max_{43} = I_{43}^1$ corresponds to the first peak of $\bar{d}I_{43}$.

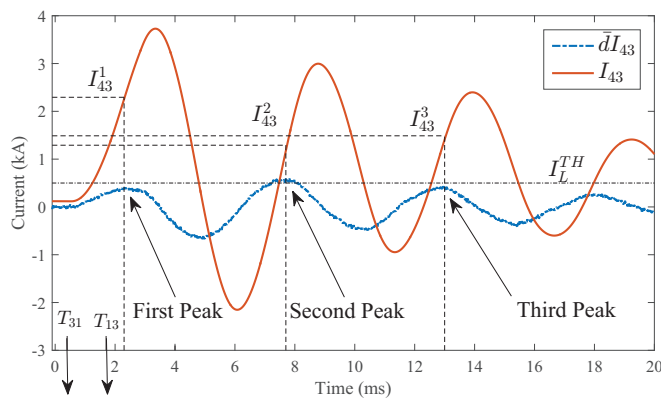


Fig. 16: $\bar{d}I_{43}$ and I_{43} during the pole-to-pole F_{311} fault

In the proposed relaying algorithm, the breaker coordination module is developed to further improve the protection system reliability. $\bar{d}I_{ij}$ signals associated with healthy lines connected

to the bus closest to the fault location may eventually experience large positive peaks as the fault wave travels back toward the fault location. As an example, $\bar{d}I_{34}$, which primarily has a negative peak, reaches 0.7 kA, Fig. 17. The breaker coordination module ensures this positive peak does not lead to CB_{34} trip. Since the breaker coordination module of each bus does not allow the trip of more than one breaker connected to a bus, T_{34} remains zero as T_{31} has already become one. This feature can be achieved as communication at the bus level is possible in the proposed algorithm.

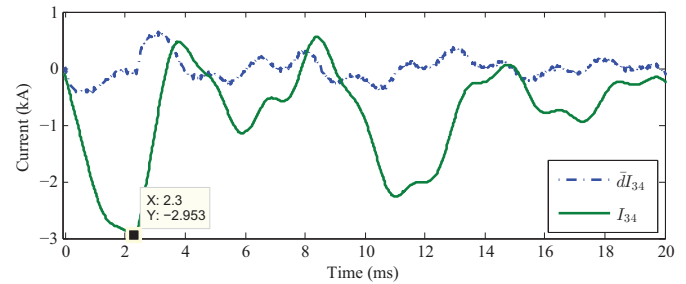


Fig. 17: $\bar{d}I_{34}$ and I_{34} during the pole-to-pole F_{311} fault

2) *Line Outage*: To remove line L_{13} , the breakers at the two ends of the line are opened at 1 ms. Fig. 18 shows that the line outage does not cause any breaker trips and only results in a change of steady-state currents.

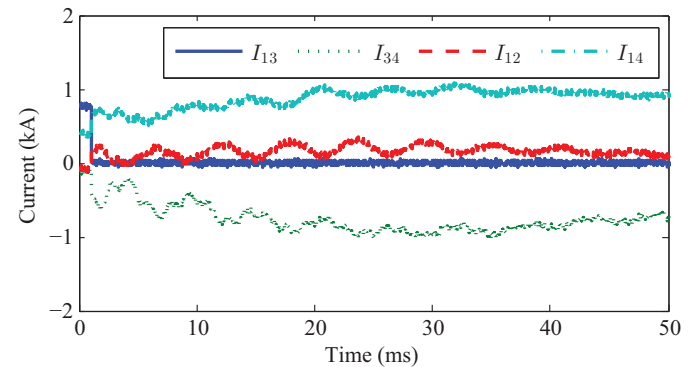


Fig. 18: Current measurements of the lines adjacent to line L_{13} after L_{13} outage

3) *Converter Outage*: Fig. 19 shows the current measurements after converter 3 outage at 1 ms. After the disconnection of converter 3 by opening CB_3 , the rest of breakers remain closed and the line currents reach their new steady-state values. Fig. 19 confirms that the proposed algorithm distinguishes between transients caused by faults and system outages.

V. DISCUSSION ON THE ROLE OF INDUCTORS IN FAULT DISCRIMINATION

In most AC-DC systems, inductors are placed in series with breakers to limit the rate of rise of current. As an example, in [13], hybrid breakers proposed in [23] are used along with inductors.

In algorithms based on current measurements, the inductors are not required to detect bus faults. In case of line faults,

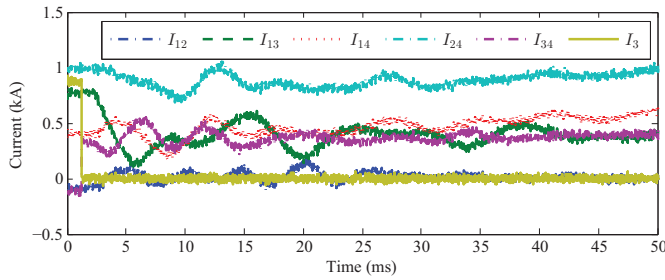


Fig. 19: Positive pole current measurements of all system lines after converter 3 outage

the inductors are required for the relay at the remote end of a longer transmission line to detect the fault. As an example, if a fault occurs on L_{14} close to bus 1, CB_{14} is the first to trip. CB_{12} and CB_{13} will not trip because they are connected to the same bus as CB_{14} . However, since the proposed algorithm does not use communication, the trip signal cannot be sent to breaker CB_{41} to remove the faulty line. Albeit, the relay at bus 4 should detect the fault on line L_{14} and send the trip signal to CB_{41} . There is a possibility that CB_{21} trips before CB_{41} as the fault current passing through S_{21} and S_{41} is positive and increasing, furthermore, the length of transmission line L_{12} is shorter than L_{14} and the fault wave reaches bus 2 before bus 4. However, due to the inductors in the system, the rate of rise of current in L_{12} is lower than L_{14} as there are two and one inductors in the fault paths, respectively. The larger the inductors, the easier to distinguish the faulty line. This is not limited to the proposed algorithm as the reported algorithms (without communication) in literature such as the one in [12], [13] also consider the inductors. If a fault occurs on a shorter line, there would be no issue for the relay at the remote end to detect the fault before other relays (selectivity is achieved).

VI. CONCLUSION

This paper proposes a fast local bus primary relaying algorithm for HVDC grids to i) detect faults on DC terminals and transmission lines and ii) identify the faulted line or bus. The key feature of the proposed algorithm is that it uses only current measurements for fault detection and identification and relies only on communication at the bus level rather than system level. The proposed algorithm satisfies the main requirements for any relaying algorithm including selectivity, sensitivity, reliability and high speed. Furthermore, the proposed algorithm is computationally inexpensive and detects faults by evaluating a number of simple criteria. The proposed relaying algorithm discriminates between faults and other system disturbances and does not lead to unnecessary breaker trips due to transients caused by events other than faults.

Simulation results show that after the fault wave reaches the sensors, the proposed relaying algorithm detects DC faults both on buses and transmission lines in less than 0.5 ms. Furthermore, the trip of breakers associated with the faulted bus or transmission line does not trigger the unnecessary trip of other breakers.

ACKNOWLEDGMENT

The research leading to these results has received funding from the People Programme (Marie Curie Actions) of the European Union's Seventh Framework Programme FP7/2007-2013/ under REA grant agreement no. 317221, project title MEDOW.

REFERENCES

- [1] ENTSO-E. (2012, Jul.) Ten-year network development plan 2012. [Online]. Available: <https://www.entsoe.eu/publications/major-publications/Pages/default.aspx>
- [2] D. Van Hertem and M. Ghandhari, "Multi-terminal VSC HVDC for the European supergrid: Obstacles," *Renewable and Sustainable Energy Reviews*, vol. 14, no. 9, pp. 3156 – 3163, 2010.
- [3] C. Franck, "HVDC circuit breakers: A review identifying future research needs," *IEEE Trans. Power Del.*, vol. 26, no. 2, pp. 998–1007, 2011.
- [4] J. Descloux, "Protection contre les courts-circuits des réseaux à courant continu de forte puissance," Ph.D. dissertation, Université de Grenoble, Grenoble, France, Sep. 2013.
- [5] S. L. Blond, R. B. Jr., D. Coury, and J. Vieira, "Design of protection schemes for multi-terminal HVDC systems," *Renewable and Sustainable Energy Reviews*, vol. 56, pp. 965 – 974, 2016. [Online]. Available: <http://www.sciencedirect.com/science/article/pii/S1364032115014082>
- [6] D. Naidoo and N. M. Ijumba, "HVDC line protection for the proposed future HVDC systems," in *Power System Technology (POWERCON), International Conference on*, Singapore, 2004, pp. 1327–1332.
- [7] D. Jovcic, D. van Hertem, K. Linden, J. P. Taisne, and W. Grieshaber, "Feasibility of dc transmission networks," in *Innovative Smart Grid Technologies (ISGT Europe), 2011 2nd IEEE PES International Conference and Exhibition on*, Dec 2011, pp. 1–8.
- [8] J. Descloux, B. Raison, and J.-B. Curis, "Protection algorithm based on differential voltage measurement for MTDC grids," in *Proc. IET DPSP 2014*, 31 Mar.-3 Apr. 2014, 5.
- [9] M. Bucher and C. Franck, "Contribution of fault current sources in multiterminal HVDC cable networks," *IEEE Trans. Power Del.*, vol. 28, no. 3, pp. 1796–1803, 2013.
- [10] M. E. Baran and N. R. Mahajan, "Overcurrent protection on voltage-source-converter-based multiterminal dc distribution systems," *IEEE Trans. Power Del.*, vol. 22, no. 1, pp. 406–412, Jan 2007.
- [11] Y. Zhang, N. Tai, and B. Xu, "Fault analysis and traveling-wave protection scheme for bipolar HVDC lines," *IEEE Trans. Power Del.*, vol. 27, no. 3, pp. 1583–1591, July 2012.
- [12] W. Leterme, J. Beerten, and D. Van Hertem, "Non-unit protection for hvdc grids with inductive cable termination," *IEEE Trans. Power Del.*, vol. 31, no. 2, pp. 820–828, April 2015.
- [13] J. Sneath and A. Rajapakse, "Fault detection and interruption in an earthed hvdc grid using rocov and hybrid dc breakers," *IEEE Trans. Power Del.*, vol. PP, no. 99, pp. 1–1, 2014.
- [14] J. Yang, J. Fletcher, and J. O'Reilly, "Multiterminal dc wind farm collection grid internal fault analysis and protection design," *IEEE Trans. Power Del.*, vol. 25, no. 4, pp. 2308–2318, 2010.
- [15] J. Zhang, J. Suonan, Z. Jiao, G. Song, and X. Su, "A fast full-line tripping distance protection method for HVDC transmission line," in *ASIA-PACIFIC POWER AND ENERGY ENGINEERING CONFERENCE*, Shanghai, 2012.
- [16] M. Bollen, "On travelling-wave-based protection of high-voltage networks," Ph.D. dissertation, TU Eindhoven, Eindhoven, The Netherlands, 1989.
- [17] M. Chamia and S. Liberman, "Ultra high speed relay for ehv/uhv transmission lines – development, design and application," *IEEE Trans. Power App. Syst.*, vol. PAS-97, no. 6, pp. 2104–2116, Nov 1978.
- [18] M. Hajian, L. Zhang, and D. Jovcic, "DC transmission grid with low speed protection using mechanical DC circuit breakers," *IEEE Trans. Power Del.*, vol. 30, no. 3, pp. 1383–1391, 2014.
- [19] A. E. Abu-Elanien, A. A. Elserougi, A. S. Abdel-Khalik, A. M. Massoud, and S. Ahmed, "A differential protection technique for multi-terminal HVDC," *Electric Power Systems Research*, vol. 130, pp. 78 – 88, 2016. [Online]. Available: <http://www.sciencedirect.com/science/article/pii/S0378779615002588>
- [20] L. Tang and B. Ooi, "Locating and isolating dc faults in multi-terminal dc systems," *IEEE Trans. Power Del.*, vol. 22, no. 3, pp. 1877–1884, Jul. 2007.

- [21] W. Leterme, N. Ahmed, L. Ängquist, J. Beerten, D. Van Hertem, and S. Norrga, "A new HVDC grid test system for HVDC grid dynamics and protection studies in EMTP," in *Proc. IET ACDC 2015*, Birmingham, UK, 10 Feb.-12 Feb. 2015, 6 pages.
- [22] N. Ahmed, L. Ängquist, S. Norrga, and H.-P. Nee, "Validation of the continuous model of the modular multilevel converter with blocking/deblocking capability," in *Proc. IET ACDC 2012*, Birmingham, UK, 4-6 Dec. 2012, 6 pages.
- [23] J. Häfner and B. Jacobson, "Proactive Hybrid HVDC Breakers: A key innovation for reliable HVDC grids," in *CIGRÉ Bologna Symp.*, Bologna, Italy, 13- 15 Sep. 2011, 8 pages.
- [24] PSCAD. (2010) EMTDC User Guide. [Online]. Available: <https://hvdc.ca/knowledge-library/reference-material>

Sahar Pirooz Azad received the Ph.D. degree in electrical engineering from the University of Toronto in 2013. She was a post-doctoral fellow at University of Toronto and KU Leuven in 2014 and 2015, respectively. She is currently an Assistant Professor at the University of Alberta. Her areas of interest include HVDC systems as well as power systems control and protection.

Dirk Van Hertem (S'02-SM'09) received his Ph.D. degree from KU Leuven in 2009. In 2010, he was a member of EPS group at the Royal Institute of Technology, in Stockholm, Sweden. Since spring 2011 he is back at the University of Leuven where he is an Assistant Professor in the Electa group. His special fields of interest are power system operation and control in systems with FACTS and HVDC and building the transmission system of the future, including offshore grids and the supergrid concept. He is an active member of IEEE PES and IAS and Cigré.